Prognostic value of integrin αV expression and localization pattern in invasive breast carcinomas

Otto Luiz Dutra Cerqueira [a,c];
Mayara Carolline Silva Botelho [a];
Ana Paula Zen Petisco Fiore [a];
Cynthia Aparecida Bueno de Toledo Osório [b];
Rebeka Tomasin [a]; Mauro César Cafundó Morais [c];
Rossana Verónica Mendoza López [c];
Elaine Cristina Cardoso [d];
Santiago Andres Vilella-Arias [a];
Eduardo Moraes Reis [a,*]; Alexandre Bruni-Cardoso [a,*]

[a] Departamento de Bioquímica, Instituto de Química, Universidade de São Paulo, São Paulo, SP, 05508-900, Brasil
[b] Department of Pathology, A.C. Camargo Hospital, São Paulo, SP, 01509-900, Brazil
[c] Centro de Investigação Translacional em Oncologia, Instituto do Câncer do Estado de São Paulo (ICESP), Hospital das Clínicas HCFMUSP, Faculdade de Medicina, Universidade de São Paulo, São Paulo, SP, 01246-000, Brazil
[d] Department of Pediatrics Laboratory of Medical Investigation, School of Medicine, Universidade de São Paulo, São Paulo, SP, 1246-000, Brazil

Abstract

Invasion of surrounding stroma is an early event in breast cancer metastatic progression, and involves loss of cell polarity, loss of myoepithelial layer, epithelial-mesenchymal transition (EMT) and remodeling of the extracellular matrix (ECM). Integrins are transmembrane receptors responsible for cell-ECM binding, which triggers signals that regulate many aspects of cell behavior and fate. Changes in the expression, localization and pairing of integrins contribute for abnormal responses found in transformed epithelia. We analyzed 345 human breast cancer samples in tissue microarrays (TMA) from cases diagnosed with invasive breast carcinoma to assess the expression and localization pattern of integrin αV and correlation with clinical parameters. Patients with lower levels of integrin αV staining showed reduced cancer specific survival. A subset of cases presented a peripheral staining of integrin αV surrounding tumor cell clusters, possibly matching the remaining myoepithelial layer. Indeed, the majority of ductal carcinoma *in situ* (DCIS) components found in the TMA presented integrin αV at their periphery, whereas this pattern was mostly lost in invasive components, even in the same sample. The lack of peripheral integrin αV correlated with decreased cancer specific survival. In addition, we observed that the presence of integrin αV in the stroma was an indicative of poor survival and metastatic disease. Consistently, by interrogating publicly available datasets we found that, although patients with higher mRNA levels of integrin αV had increased risk of developing metastasis, high co-expression of integrin αV and a myoepithelial cell marker (MYH11) mRNA levels correlated with better clinical outcomes. Finally, a 3D cell culture model of non-malignant and malignant cells reproduced the integrin αV pattern seen in patient samples. Taken together, our data indicate that both the expression levels of integrin αV and its tissue localization in primary tumors have prognostic value, and thus, could be used to help predict patients at higher risk of developing metastasis.

* Corresponding authors at: Alexandre Bruni-Cardoso and Eduardo Moraes Reis, Departamento de Bioquímica, Instituto de Química, Universidade de São Paulo, São Paulo, SP, 05508-900, Brazil, Tel: +55 1130919047
E-mail addresses: emreis@iq.usp.br (E.M. Reis), brunicar@iq.usp.br (A. Bruni-Cardoso).

Introduction

The vast majority of breast cancer deaths are due to metastatic disease [1]. Many patients might bear occult metastatic disease at the time of diagnosis, therefore, the identification of specific characteristics in the primary tumor, that could predict whether the disease is more likely to metastasize, would contribute to better stratify the patients and perhaps change the therapeutic strategy.

In cancer, the bidirectional exchange of biochemical and mechanical information between epithelial cells and the extracellular matrix (ECM) – which is crucial for cell survival, tissue architecture and organ function – is aberrant [2]. The cell-ECM communication is mediated mainly by heterodimers of integrins, integral membrane proteins that bind to ECM molecules outside of cells and to cytoskeleton and signaling proteins in the cytoplasm [3–5]. One overt trait of cancer, largely used for diagnosis, is the loss of tissue architecture. During breast cancer progression, the epithelial architecture found in the mammary gland is compromised, presenting a progressive loss of cell polarity and a reduction in the number of myoepithelial cells [6]. These events are frequently accompanied by changes in integrin expression and different combinations of integrin heterodimers, which contribute for dysfunctions in cell adhesion, survival and proliferation, as well as for anoikis resistance and increased invasive behavior found in cancer cells [7–10].

A previous study conducted by our group sought at identifying biomarkers for breast cancer prognosis. By analyzing gene expression profiles of a set of invasive ductal carcinoma primary tumor samples, we identified 58 transcripts capable of discriminating groups of patients who had developed or not metastases within the 5-year postoperative period [11]. Among these genes, *ITGAV,* that encodes integrin αV (also known as CD51; Cluster of differentiation 51), was overexpressed in tumors from patients who evolved to metastatic disease. Integrin αV has some peculiarities when compared with other integrins: while most alpha integrin subunits generally can only dimerize with one specific β subunit, integrin αV can bind to five different β subunits [12] and the resulting heterodimers recognizes a variety of ECM ligands, including vitronectin and fibronectin [3,13]. Moreover, integrin αV, as well as its heterodimers, are important targets for the development of therapeutic strategies for solid and hematologic tumors [12].

In this study, we investigated the expression and localization pattern of integrin αV in a cohort of 345 invasive breast cancer samples from patients with known follow-up and clinical information. By performing immunohistochemistry (IHC) on tissue microarrays (TMA), we found striking differences in the staining pattern of integrin αV. While integrin αV was preferentially localized at the periphery of ductal carcinoma *in situ* (DCIS) components, this pattern was lost in the invasive component. We also found that loss of integrin αV in the periphery of neoplastic lesions might predict poor cancer-specific survival. The aforementioned pattern, with loss of peripheric staining of integrin αV in more aggressive/advanced tumors, could be reproduced in three-dimensional (3D) culture assays of malignant human breast cells. Furthermore, our data indicated that the presence of integrin αV in the stroma correlated with poor survival and higher probability of metastatic disease. Thus, our findings highlight the localization pattern of integrin αV as a putative biomarker for breast cancer prognosis, and provide a model for investigating the role of this integrin in breast cancer biology.

Material and methods

Patient samples and clinical data

The patient's cohort was diagnosed and treated in A.C. Camargo Cancer Center, São Paulo, Brazil and clinical follow-up was registered until 2008. A total of 345 cases of invasive breast carcinoma primary tumors were used in this study. Although all the patients in the cohort were diagnosed as having invasive breast carcinoma, in 35 cases we could find DCIS components in the Tissue Microarray (TMA) sections. None of the patients included in our study received neo-adjuvant chemotherapy. The procedure for collection of cancer surgical specimens, paraffin embedding and TMA block preparation has been previously described [14,15]. Briefly, each tissue sample was thoroughly inspected by a pathologist who selected a morphologically representative region of the sample that was subsequently placed in a TMA master block using a Beecher Tissue Microarrayer Instrument (Beecher Instruments, Silver Spring, MD). Sections of TMA were transferred to glass slides and subsequently stained for integrin αV by IHC. This study was registered and approved by the local institutional ethics committee, CIPE-Centro Internacional de Pesquisa e Ensino-A.C. Camargo Cancer Center, with protocol number 1822/13. All patients agreed with an informed consent document.

Immunohistochemistry and TMA analysis

Immunohistochemistry reactions were performed in the Laboratory of Pathology Research at AC Camargo Cancer Center by a trained technician as previously described [14,15]. Briefly, sections from the TMA blocks were deparaffinized, rehydrated, subjected to antigen retrieval, inactivation of tissue peroxides and blockage. TMA slides were then incubated overnight with anti-integrin αV (sc-9969, Santa Cruz Biotechnology Inc.) at 1:250. Mouse secondary antibody HRP (Horseradish peroxidase) coupled dextran polymer detection system (Advance TM HRP link - Dako) was incubated for 30 min at room temperature after standard washes accordingly to manufacturer recommendations. Finally, the presence of integrin αV was detected by addition of 3,3′-diaminobenzine tetrachloride (FLEX DAB+ Substrate Chromogen System, Dako) to the samples. TMA slides were counterstained with Meyer hematoxylin and scanned in a ScanScope AT Turbo image capture system (Aperio ePathology Solution Inc.).

Samples were analyzed by a pathologist (C.A.B.T.O.), blinded for the clinic-pathological variables. We assessed integrin αV expression in the TMA in 4 different levels: i) total integrin αV levels based on H-Score, ii) integrin αV staining at the periphery (epithelium-stroma interface) of tumor cell clusters, iii) integrin αV staining at the membranes of individual cells, and iv) integrin αV staining in stroma.

Total integrin αV quantification was performed using the automatic "Pixel Count V9" algorithm from the Imagescope software (Aperio ePathology Solutions Inc) as previously described [14]. The software was set for detection of DAB immunostaining without interference of Meyer hematoxylin stain. For each sample, final H-Score values were calculated and ranged from 0 (no staining) to 300 (100% of tumor cells strongly stained). This approach allows assessment of the intensity of IHC staining in tumor areas previously selected by the program user to determine the global levels of the protein but does not allow detection of subcellular staining variations [14] . However, through visual inspection, we noticed in some samples that integrin αV had a defined marginal distribution patterns around tumor cell clusters at the interface with the stroma, that we here termed as peripheral integrin αV. There are no established pathological guidelines or validations for the quantification of proteins at the periphery of tumor cell clusters. We, therefore, relied on previous studies that also assessed the level and localization patterns of proteins at the borders of neoplastic cell clusters and the adjacent stroma [16–19]. For quantification of peripheral integrin αV, we defined the following score: 0-Negative, 1-Weak, 2-Moderate and 3-Strong, which was based on the intensity of the immunohistochemical staining at the epithelium-stroma borders. Likewise, stromal integrin αV also lacks guidelines for quantification by IHC. We relied on visual parameters to measure the intensity of integrin α immunostaining in the stroma based on the routine experience of the pathologist C.A.B.T.O. in breast cancer, as well other tumors, blinded to the anatomopathological data. Initially, we determined stromal staining using the score: 0-Negative, 1-Weak, 2-Moderate

and 3-Strong. For all survival curves, we only considered Negative (score 0) x Positive, which aggregates samples with scores 1-Weak, 2-Moderate and 3-Strong. For integrin αV membrane staining quantification, we used the same recommendation of ASCO guidelines used for HER2 [20].

Statistical analysis

Statistical analyses were performed using Graph Pad Prism 5.0 (Graph Pad Software Inc.) and SPSS v.18 for Windows. Chi-square test was used in cross-tabulation analysis to evaluate significant associations between integrin αV peripheral staining and clinico-pathologic variables. Univariate Kaplan-Meier (KM) survival curves of a 10-year period were used to estimate overall survival (OS), cancer specific survival (CSS), disease-free survival (DFS) and distant disease-free survival (DDFS), which refers to the probability of patients to remain metastasis-free. Log-rank (Mantel-Cox) test was used to assess difference between survival curves. For DDFS and DFS, we censored patients who already had metastasis at the time of diagnosis. Prognostic factors were evaluated by Cox regression model with 95% confidence intervals. A significance level of 0.05 was considered for all statistical analyses.

Cell lines

Human breast cell lines were gently donated by Mina J. Bissell from the Lawrence Berkeley National Laboratory. The cancer cell lines MCF-7 (luminal) and MDA-MB-231 (basal-like) cells were grown in Dulbecco's Modified Eagle Medium, (DMEM Invitrogen) with 10% fetal bovine serum (Invitrogen) and the non -malignant MCF-10A cells were grown in DMEM/F-12 (Invitrogen) with 10 ng/mL insulin, 100 ng/mL cholera toxin, 500 ng/mL hydrocortisone, 20 ng/mL Epidermal growth factor (Sigma), and 5% horse serum (Invitrogen). All cells were kept in a humidified 5% CO_2 incubator at 37°C and cultured until 70% confluence before subculture or protein extraction.

Protein extraction, SDS-PAGE and immunoblotting

Cells were washed twice with ice cold PBS pH7.4, and harvested by scraping in ice cold modified RIPA buffer (50 mM HEPES pH 7.4, 150 mM NaCl, 10% glycerol, 1% Triton X-100, 10 mM sodium pyrophosphate containing 1.5 mM $MgCl_2$, 1 mM EGTA, 1% sodium deoxycholate), containing protease (Complete, Roche) and phosphatase inhibitors (Phosphatase inhibitor cocktail 2, Sigma-Aldrich). Protein concentration was determined by colorimetric assay (DC Protein Assay kit, BioRad). Fifteen μg of total protein extracts were mixed with 2x Laemmli sample buffer (4% SDS, 20% glycerol, 10% 2-mercaptoethanol, 0.004% bromophenol blue and 0.125 M Tris HCl, pH 6.8) and heated at 95°C for 5 minutes. Protein samples were loaded into 8% SDS-PAGE (sodium dodecyl sulfate–polyacrylamide gel electrophoresis) and resolved proteins were transferred to a PVDF membrane (Millipore) followed by blocking in Tris-Buffered Saline containing 0.5% Tween-20 (TBS-T) with 5% bovine serum albumin (BSA). Membranes were incubated overnight in TBS-Tween 1% BSA containing primary antibodies. Primary antibodies (anti-integrin αV, #611435, BD Biosciences and anti-beta Actin, AM4302, Life Technologies) were recognized by mouse or rabbit HRP conjugated secondary antibodies (115-035-174, Jackson ImmunoResearch and 32460, Invitrogen) and the bands were detected using an enhanced chemiluminescent system (SuperSignal detection kit, from Thermo). Chemiluminescence signal was captured with an Uvitec Aliance analysis system (Uvitec Cambridge), each band integrated optical density was determined by Image J (1.37v Software, NIH Public Domain, USA), and then normalized to β-actin before fold-change determination.

Three-dimensional culture and immunofluorescence

Three-dimensional (3D) cultures were performed by seeding single cells (after trypsinization) on PolyHEMA-coated plates (0.8 mg/cm^2, Sigma-Aldrich). MCF-10A cells were seeded at a density of 3×10^4 cells per cm^2; MCF-7 cells were seeded at 2×10^4 cells per cm^2; and MDA-MB-231 were seeded at 1.5×10^4 cells per cm^2. All 3D cell cultures were maintained for 10 days in H14 medium (DMEM/F-12 medium, containing 250 ng/mL insulin, 10 μg/mL transferrin, 2.6 ng/mL sodium selenite, 10 μM estradiol, 1.4×10^{-6} M hydrocortisone, 5 μg/mL prolactin, 10 ng/mL epidermal growth factor (EGF), all additives from Sigma-Aldrich) supplemented with 1% fetal bovine serum and 4% Growth-Factor Reduced Matrigel (Corning), as previously described [21].

The multicellular 3D structures were collected and transferred to glass slides, then fixed with 4% paraformaldehyde (PFA) (Electron Microscopy Sciences) in PBS pH 7.4. Residual PFA reactivity was quenched with PBS–25 mM glycine, and cells were permeabilized with 0.5% Triton X-100 in PBS for 30 minutes. The cells were then incubated in blocking buffer (1% Bovine Serum Albumin and 5% goat-serum in PBS) for 1 hour at room temperature, followed by overnight incubation with primary antibody for integrin αV (Dilution 1:250, #sc-9969, Santa Cruz Biotechnology Inc.) in blocking buffer. Cells were then incubated in blocking buffer with Alexa488 conjugated mouse secondary antibodies (#A11001, Invitrogen) for 45 min. The structures were counterstained with 4'6-diamidino-2-phenylindole (DAPI) for 10 minutes, mounted with Prolong® Gold (P36934 from Life Technologies) and imaged on a Leica DMi8 wide field microscope.

Image stacks were captured with a 40x/0.8 objective (Leica) using optimized settings and submitted to blind deconvolution with the Leica Application Suite-X software (Leica Microsystems). Image quantification of integrin αV-labeled 3D structures was performed with ImageJ (2.0.0-rc-68/1.52e; Java 1.8.0_66 64-bit) [22], using a customized macro (available upon request). In brief, spheroids were cropped from each image and integrin αV intensity was measured in 180 transverse profiles, with 1° rotation each, at the middle plane for each 3D structure, allowing the assessment of integrin αV distribution within all the perimeter of the 3D structures. The profile widths were normalized to compensate for the different sizes amongst different 3D structures and were plotted against the average integrin αV intensity showing the protein distribution in arbitrary units (A.U.).

Bioinformatics analysis using publicly available datasets

We used two publicly available platforms (Genevestigator [23] and BreastMark [24]) to further explore the significance of integrin αV expression in breast cancer cell lines and human tumors. In order to assess *ITGAV* mRNA expression levels in the cell lines used in this work (MCF-10A, MCF-7 and MDA-MB-231), we used Genevestigator [23], a high performance search tool that integrates a large number of manually curated, well described publicly available transcriptome datasets. For the present study, we used data generated with the Affymetrix Human Genome U133 Plus 2.0 Array platform. For analyzing cell lines, only samples not subjected to treatments were included.

To assess the prognostic value of *ITGAV* and *MYH11* (smooth muscle myosin heavy chain 11, a breast myoepithelial cell marker) *mRNA* levels, we used BreastMark - an algorithm freely available online that integrates published gene expression data from microarrays (corresponding to ∼17,000 genes and 341 miRNAs) and detailed clinical outcome data for breast cancer (available at: http://glados.ucd.ie/BreastMark/index.html) [23]. We evaluated the influence of high or low mRNA expression levels (using median cutoff) of *ITGAV* and *MYH11* in the Overall survival (OS), Disease-free survival (DFS) and Distant disease-free survival (DDFS), which we consider as metastasis-free survival, of over 2000 breast cancer patients. In addition to the evaluation of both genes separately, BreastMark allowed us to compare the
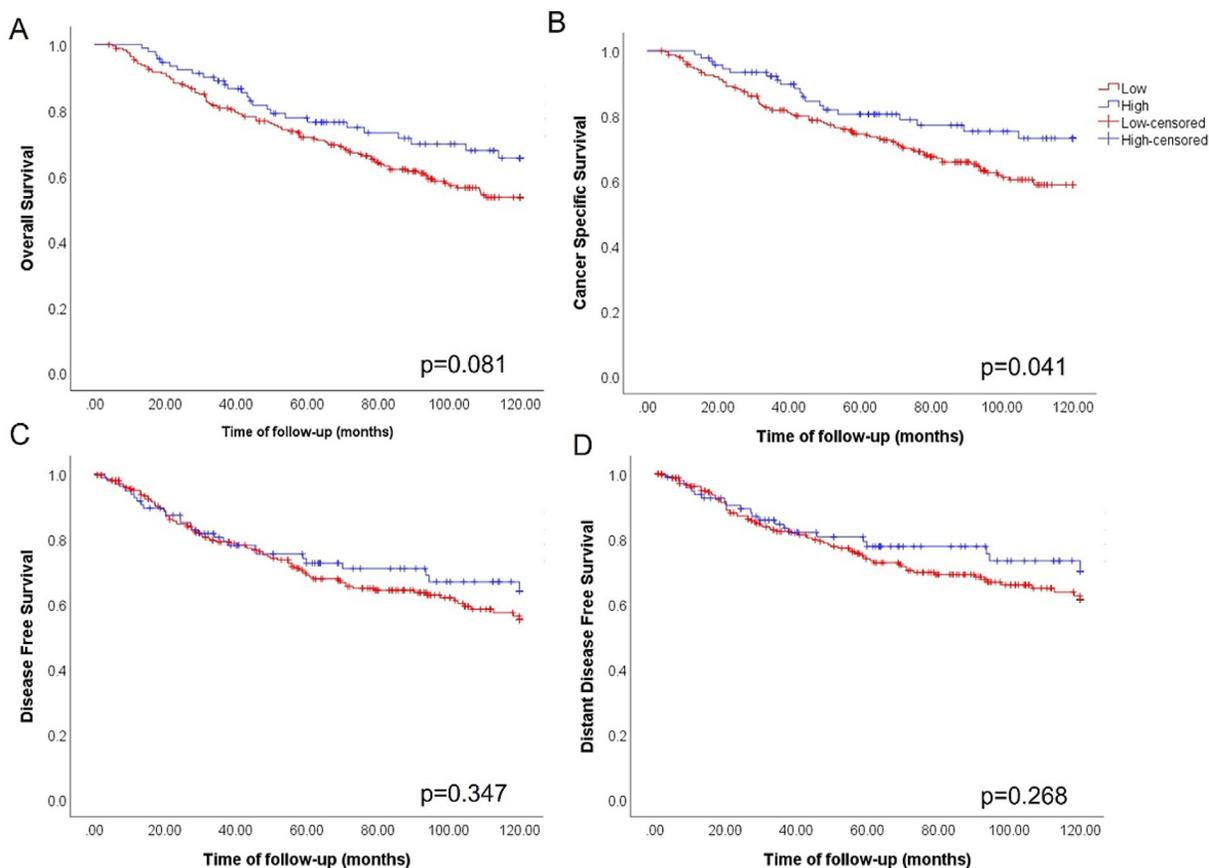
Fig. 1. Low expression of integrin αV in breast cancer tissues is linked to poor prognosis. Patients were stratified according to the expression of integrin αV: H-score under mean (= 10.34) was considered low (n=242, red) and H-score above mean, high (n=92, blue). A) Although the expression of integrin αV has not shown relevance for Overall Survival (OS) (p=0.081), cancer specific survival (CSS) (B) showed statistically significant differences pointing out that the decrease in integrin αV expression correlates with a worse prognosis (p=0.041). The expression of integrin αV did not show statistically significant relationships for both C) Disease-free survival (DFS) (p=0.347) and D) Distant disease-free survival (DDFS) (p=0.268).

clinical outcomes of subset of patients whose samples had high mRNA levels of both *ITGAV* and *MYH11* versus patients whose samples had low mRNA levels of both genes. BreastMark generates Kaplan-Meier plots and calculates the hazard ratio (HR) and p value. The HR is generated using Cox regression and is related to increased expression of the marker; an HR greater than one means that higher expression levels are associated with poor prognosis and HR of less than one means it is associated with a favorable prognosis.

Results

Expression profile of integrin αV in human breast cancer correlates with patient clinical outcomes

To investigate integrin αV expression levels in human breast cancer tissues, we performed IHC using a tissue microarray (TMA). Initially, we collected information about the intensity (based on H-Score) of integrin αV immunostaining in pre-selected tumor areas using the Aperio system quantification algorithm [25]. We determined a cutoff using the mean of H-score values to group samples in low (H-score under the mean) or high (H-score above mean) integrin αV levels. Kaplan-Meier curve analysis was performed considering this H-score cutoff and patient outcome data. We observed that patients with lower integrin αV expression had a worse prognosis for cancer specific survival (CSS) (Fig. 1). However, we found no significant correlation with the expression of integrin αV

and overall survival (OS), disease-free survival (DFS) and distant disease-free survival (DDFS). We also considered adopting the cutoff given by the median of the H-Score values of integrin αV expression, but we did not find any statistical significance for OS, CSS, DFS and DDFS KM curves (Fig. S1). Intriguingly, visual inspection of IHC stained samples revealed that integrin αV localization in epithelial cell clusters presented different patterns according to the type of lesion (Fig. 2). In normal and hyperplastic acini, expression of integrin αV was not detected in luminal cells, but a weak immunodetection of this protein can be seen in the contour of the acini, which coincided with the localization of myoepithelial cells (Fig. 2A). Likewise, the majority of samples from patients diagnosed as having invasive breast carcinomas presenting DCIS components were positively stained for integrin αV at the periphery of the tumor cell clusters, which is consistent with the fact that the myoepithelial cells layer is preserved in these structures (Fig. 2B). In contrast, this staining pattern is lost in invasive components (Fig. 2C-D). Notably, in some invasive lesions, with an extensive disorganization of the epithelial architecture, integrin αV was detected in the membrane of individual tumor cells (Fig. 2D).

Integrin αV is present in the periphery of in situ *components in patient samples presenting both DCIS and invasive components*

In our cohort, we have identified eight cases which had well-defined DCIS lesions neighboring invasive clusters in the same microscope image of a TMA core (Fig. 3A). This allowed direct comparison of peripheral integrin
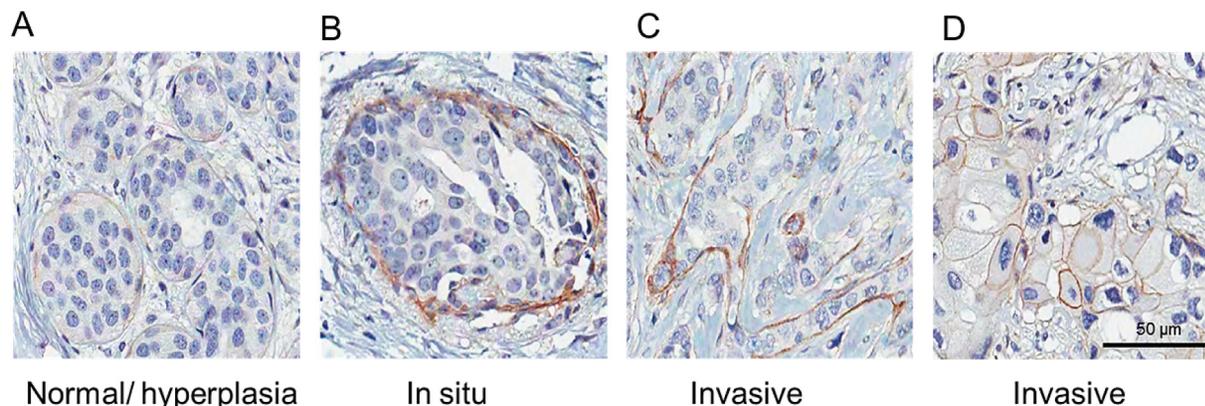
Fig. 2. Representative immunohistochemistry staining for integrin αV in different breast samples. Breast tissue sections of different types of lesions submitted to immunohistochemistry for integrin αV. Normal acini and ductal hyperplasia (A) and *in situ* component (B) display integrin αV at the lesion peripheries. C and D, invasive ductal carcinoma (IDC). In D, integrin αV can be observed contouring individual cells. Scale bar= 50 µm.

αV detection between the invasive and the DCIS components in the same patient. Compiled information regarding the presence of peripheral integrin αV in the *in situ* components versus their respective invasive components are presented in Fig. 3B. Remarkably, seven out of eight samples presented peripheral integrin αV staining at the *in situ* lesions (scored 1 or 2), whereas none of the invasive components showed this pattern (all scored 0). These findings encouraged us to investigate whether peripheral integrin αV had prognostic value.

Loss of peripheral integrin αV expression is associated with poor prognosis in invasive breast carcinomas

We analyzed whether the presence of integrin αV at the border of tumor lesions (peripheral integrin αV) would be associated to survival rates and metastasis incidence. Kaplan-Meier survival analyses were performed for overall survival (OS), cancer specific survival (CSS), disease-free survival (DFS) and distant disease-free survival (DDFS) according to the status of peripheral integrin αV for the entire cohort. Out of the 345 cases, 239 (67.3%) were negative for peripheral integrin αV, whereas 116 (32.7%) were positive. No statistically significant differences were observed in OS between patients with different peripheral integrin αV status (p=0.164; Fig. 4A). However, CSS analysis revealed that patients that lost peripheral integrin αV had a higher incidence of death related to the disease (p=0.042; Fig. 4B). An analysis of DFS showed that patients with negative status for peripheral integrin αV could be more likely to recidivate, although without statistical significance (p=0.060; Fig. 4C). No significant differences were detected between the groups with or without peripheral integrin αV in DDFS analyses (p=0.439; Fig. 4D). We also assessed the possible prognostic value of integrin αV localized in the cell membrane of individual cells, but did not find significant correlations with patient survival (Fig. S2).

To extend the analysis regarding peripheral integrin αV as a prognostic marker in breast cancer, we searched for associations with other clinicopathological parameters, displayed in (Suppl. Table 1). Univariate Chi-square association analysis were performed between peripheral and stromal integrin αV levels and the clinicopathological parameters: age, *in situ* associated lesion, Perou/Sørlie classification, ER, PR, HER2, tumor size, tumor stage, metastasis development, and vital status (Table 1).

The analysis revealed a statistically significant association between peripheral integrin αV levels and *in situ* associated, showing that 96.1% of patients without *in situ* components lost the expression of peripheral integrin αV (p = <0.001) (Table 1). Furthermore, integrin αV also correlates with HER2. Indeed, 88.2% of patients with negative peripheral integrin αV

staining were also negative for HER2 (p = 0.015) (Table 1). Vital status was also statistically significant, as 69.0% of patients alive had positive peripheral integrin αV (p = 0.018), corroborating with the data shown in Fig. 4.

Additionally, we used BreastMark to assess the clinical outcomes related to high or low integrin αV mRNA expression in large cohorts of breast cancer samples (up to 2592 cases). Our results show that integrin αV mRNA expression levels were not predictive of OS and DFS (Fig. S3 A-B). Noteworthy, high *ITGAV* mRNA levels were correlated to decreased DDFS (Fig. S3 C), as shown in a previous work from our group [11]. Because periphery integrin αV displays a similar localization to the myoepithelial cell layer, we also conducted the same analyses for *MYH11*, a breast myoepithelial cell marker. High *MYH11* was clearly linked to a better clinical outcome for OS, DFS and DDFS (Fig. S4 A-C). Finally, comparing the clinical outcome for high mRNA co-expression for both integrin αV and *MYH11* versus other co-expression patterns (high αV and low *MYH11*, low αV and low *MYH11* or low αV and high *MYH11*), high co-expression levels were significantly correlated to a better for OS and DFS, but not for DDFS (Fig. S5 A-C).

Integrin αV subcellular localization in breast cell lines cultured on 2D and in 3D resembles clinical observations

After verifying the clinical relevance of integrin αV levels and localization for human breast cancer, we pursued a relevant culture model that could reproduce our clinical findings. First, we verified the distribution and abundance of integrin αV in three human breast cell lines: MCF-10A (nonmalignant), MCF-7 (luminal cancer) and MDA-MB-231 (basal-like cancer). Integrin αV was detected in all three cell lines, albeit MDA-MB-231 cells presented 50% less of integrin αV when compared to MCF-10A cells, as assessed by western blotting (Fig. 5A). This is partially consistent with integrin αV mRNA expression levels for these cell lines according to the data available of Genevestigator [23], which indicates progressive loss of integrin αV in the malignant cells (Fig. 5B). In addition, we evaluated the subcellular distribution of integrin αV in the different cell lines cultured as monolayers. Immunofluorescence analysis from the cell lines collected in the same experimental conditions corroborated the western blot results. MDA-MB-231 cells exhibited lower levels of integrin αV and, importantly, integrin αV was fainter at the membrane of these highly aggressive malignant cells (Fig. 5C).

Because integrins are critical molecules bridging cells with their surroundings, we decided to evaluate the localization of integrin αV in cells cultured in a 3D environment in the presence of a reconstituted basement membrane (rBM; Matrigel). The cells were cultured for 10 days; a time-

A

B
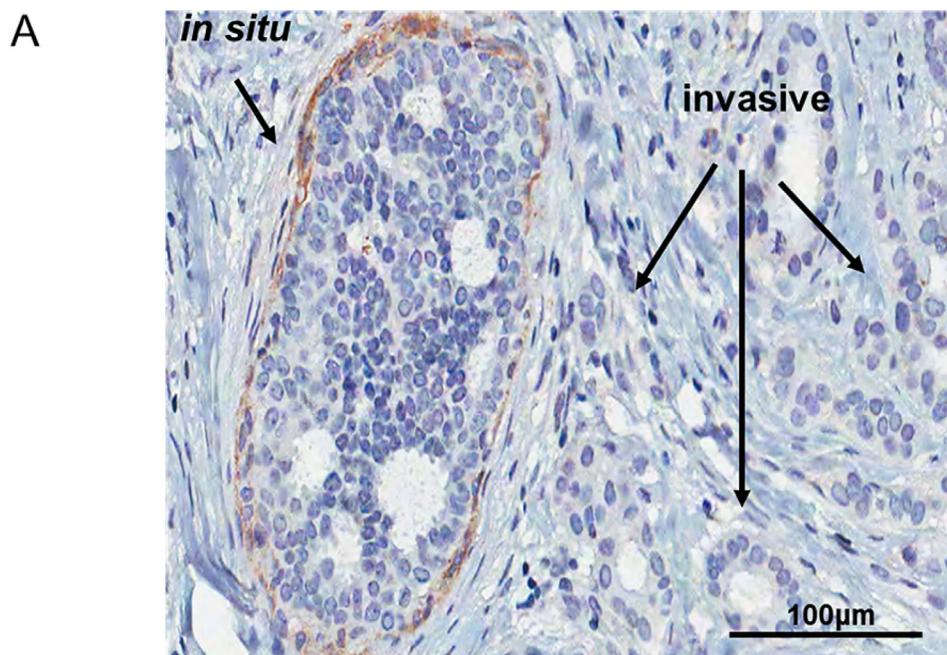
					Peripheral ITGAV score	
case	ER	PR	HER2	subtype	*in situ* component	invasive component
333	-	+	-	Luminal	2	0
853	+	+	-	Luminal	2	0
1075	+	+	NA	Luminal	1	0
1081	+	+	+	Luminal	1	0
1106	+	+	-	Luminal	1	0
1177	-	-	-	Basal	1	0
1251	+	+	-	Luminal	1	0
658	+	+	-	Luminal	0	0

Fig. 3. Comparison between *in situ* and invasive components found in the same patient TMA core. (A) Representative image of an IDC case with *in situ* component, the latter displaying peripheral integrin αV. Typical *in situ* component (indicated by an arrow) outlined by integrin αV staining. The invasive component shows almost complete absence of peripheral integrin αV. Scale bar = 100 μm. See supplementary Figure 1 for an additional representative image. (B) Detailed information of 8 cases that had both *in situ* and invasive components, regarding the presence and intensity of peripheral integrin αV and molecular subtype classification.

frame long enough for the non-malignant (MCF-10A) cells to form 3D basal polarized and growth-arrested acini in this assay. In 3D cultures of rBM, MCF-7 cells form non-polarized multicellular spherical masses, while MDA-MB-231 give rise to invasive tumor-like 3D structures [21]. We observed that in non-tumoral cells breast epithelial cells (MCF-10A) integrin αV is mostly concentrated at the border of the acini, similar to the pattern seen for normal acini and DCIS components (Fig. 6A-B). On the other hand, malignant cells (MCF-7 and MDA-MB-231) presented a different pattern, with the integrin αV more evenly distributed in the 3D structures (Fig. 6A-B).

Stromal integrin αV is associated with poor prognosis in invasive breast carcinomas

Visual inspection of IHC stained samples revealed that integrin αV can also be localized in areas of the tumor stroma. Of note, we could observe an immunostaining of integrin αV dispersed in the tumor stroma in some of the samples (Fig. 7). Representative images show clear evidence that there is immunostaining for integrin αV dispersed in non cellular elements of the extracellular matrix, as well as in stromal cells. To investigate the prognostic value of stromal integrin αV, we performed Kaplan-Meier survival analysis in function of patient outcome data. We grouped patients with either negative or positive stromal integrin αV. Although with marginal significance, stromal integrin αV positivity correlated with worse OS (p=0.052) (Fig. 8A). However, for CSS, positive stromal integrin αV expression showed a strong statistical correlation with poor prognosis (p=0.017) (Fig. 8B). Additionally, we observed that patients with positive stromal integrin αV had a worse prognosis for DFS (p=0.024) (Fig. 8C), as well DDFS (p=0.036) (Fig. 8D), indicating that it may be related to the incidence of recurrence and metastases, respectively. Collectively, our data show that stromal integrin αV positivity is linked to poor prognostic indicators.
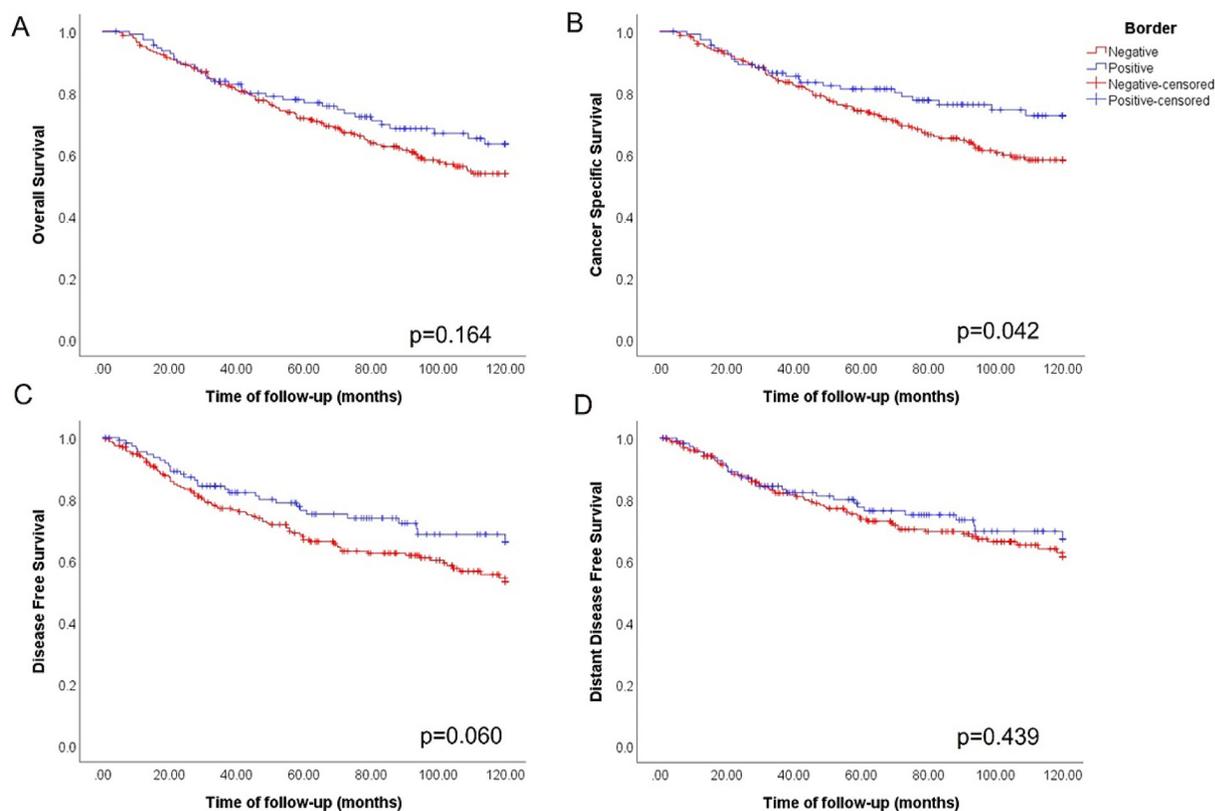
Fig. 4. Loss of peripheral integrin αV is associated with poor prognosis in human breast tumors. Kaplan-Meier survival analyses for patients with breast cancer stratified by negative (n=225, red) or positive (n=113, blue) staining for peripheral integrin αV: A) For overall survival (OS), no statistical differences were found between the groups (p=0.164). However, in B) the cancer specific survival (CSS) plot shows that patients with loss of peripheral expression of integrin αV had a worse prognosis when compared to those who maintained integrin αV in the periphery of the lesion clusters (p=0.042). For the disease-free survival (DFS) KM plot C), we did not observe statistical differences (p=0.060), although a trend of greater incidence of metastases can be observed in patients with no peripheral integrin αV. For D) Distant disease-free survival (DDFS), no significant differences were detected between the groups (p=0.439).

Discussion

Much effort has already been employed to understand differences related to integrins during tumor progression. Most studies that sought to correlate integrin with clinical outcomes have relied on measuring mRNA or protein levels [11,26-31]. We initially investigated the protein levels of integrin αV by Tissue Microarray (TMA) in a set of breast cancer samples and found statistically significant correlations between total protein levels of integrin αV and patient clinical outcomes; low expression is associated with poor prognosis with higher risk of death due to breast cancer. Intriguingly, when we assessed the correlation of integrin αV mRNA levels and clinical outcome on Breastmark, no significant differences were observed for OS or DFS. On the other hand, and consistent with our previous findings [11], we found that higher integrin αV mRNA levels were significantly associated to metastatic relapse. In fact, although a correlation between levels of mRNAs and their respective proteins could be generally expected, there is evidence in the literature indicating that there is only partial correspondence between the levels of these two entities [32–35]. There are several reasons that account for these discrepancies, including the dynamics of RNA expression and protein translation and degradation, that are independent and subject to different post-transcriptional regulatory mechanisms [36,37].

Visual inspection of the tissue slides revealed a peculiar pattern of integrin αV localization, especially at the periphery of ductal lesions *in situ*. Additional analysis revealed that the peripheral localization of integrin αV was associated to a better prognostic. We found a reduction in the immunodetection of integrin αV in the periphery of tumor cell clusters in

invasive lesions. This reduction is likely to have occurred concomitantly with the loss of the myoepithelial layer, and probably the basement membrane, once myoepithelial cells are responsible for its production [38]. The basement membrane has been shown to be a physical barrier to avoid the direct interaction between epithelial cells and the collagen-rich stroma, and to trigger intracellular pathways responsible for keeping the epithelial cells in a normal low-proliferation state [39,40]. Indeed, along with tumor progression, myoepithelial cells are not only outnumbered by cancer cells, but also become unable to produce laminin-111, a major component of the basement membrane [38]. Supporting the notion that the presence of a functional myoepithelial layer (which happens to be positively stained by integrin αV) [41] has a positive impact in clinical outcome, high levels of *MYH11* mRNA (a breast myoepithelial cell marker) were significantly correlated with increased OS, DFS and DDFS. The molecular mechanisms and cellular events underlying the transition from pure DCIS to invasive carcinoma are still elusive. Once myoepithelial cells are in direct contact with the surrounding ECM, and have a possible role in suppressing malignant lesions, changes in their gene expression profile and phenotype have been proposed as important steps for breast cancer progression [42]. Indeed, upregulation of the heterodimer integrin αVβ6 in DCIS-associated myoepithelial cells might trigger a switch in their role from tumor suppressive to tumor promoting. The biological relevance of integrin αV pairing with β-integrin subunits for the transition from non-invasive to invasive disease still needs to be addressed clinically and functionally. Intriguingly, many invasive cell clusters that have lost peripheral integrin αV display this integrin at the membrane of individual cells. Probably, invading tumor cells use this integrin

Table 1

Univariate Chi-square analysis between peripheral or stromal integrin αV levels and the clinico-pathological parameters of breast carcinoma cases

Parameter	Total (345)	Peripheral integrin αV			Stromal integrin αV		
		Negative	Positive	p-value	Negative	Positive	p-value
Age	343	230 (100%)	113 (100%)		185 (100%)	158 (100%)	
range 24 – 50		86 (37.4%)	48 (42.5%)	0.410	68 (36.7%)	66 (41.8%)	0.343
range 51 – 98		144 (62.6%)	65 (57.5%)		117 (63.3%)	92 (58.2%)	
NA/ND[b]	2						
age,		230 (66.7%)	113 (32.8%)	0.672	185 (53.6%)	158 (45.8%)	0.647
In situ associated	345	231 (100%)	114 (100%)		185 (100%)	160 (100%)	
Negative		222 (96.1%)	88 (77.2%)	<0.001	159 (85.9%)	151 (94.4%)	0.012
Positive		9 (3.9%)	26 (22.8%)		26 (14.1%)	9 (5.6%)	
NA/ND[b]	0						
SBR	333	222 (100%)	111 (100%)		176 (100%)	157 (100%)	
1		29 (13.1%)	18 (16.2%)	0.202	29 (16.4%)	18 (11.5%)	0.095
2		127 (57.2%)	70 (63.1%)		108 (61.2%)	89 (56.7%)	
3		66 (29.7%)	23 (20.7%)		39 (22.4%)	50 (31.8%)	
NA/ND[b]	12						
Perou/Sorlie Classification	326	220 (100%)	106 (100%)		174	152	
Luminal		162 (73.6%)	77 (72.6%)	0.07	131 (75.3%)	107(70.4%)	0.509
HER2+		15 (6.8%)	15 (14.2%)		16 (9.2%)	14 (9.2%)	
Basal Like		43 (19.6%)	14 (13.2%)		27 (15.5%)	31 (20.4%)	
Non characterized	19						
Estrogen receptor (ER)	333	224 (100%)	109 (100%)		177 (100%)	156 (100%)	
Negative		68 (30.3%)	34 (31.2%)	0.900	47 (26.6%)	55 (35.2%)	0.096
Positive		156 (69.7%)	75 (68.8%)		130 (73.4%)	101 (64.8%)	
NA/ND[b]	12						
Progesterone receptor (PR)	336	226 (100%)	110 (100%)		180 (100%)	156 (100%)	
Negative		118 (52.2%)	46 (41.8%)	0.082	84 (46.7%)	80 (51.3%)	0.444
Positive		108 (47.8%)	64 (58.2%)		96 (53.3%)	76 (48.7%)	
NA/ND	9						
HER2	291	196 (100%)	95 (100%)		156 (100%)	135 (100%)	
Negative		173 (88.2%)	73 (76.8%)	0.015	132 (84.6%)	114 (84.4%)	0.548
Positive		23 (11.8%)	22 (23.2%)		24 (15.4%)	21 (15.6%)	
NA/ND	54						
Tumor Size (cm)	332	224 (100%)	108 (100%)		182 (100%)	150 (100%)	
≤ 2		34 (15.2%)	23 (21.3%)	0.337	33 (18.1%)	24 (16.0%)	0.804
> 2 and ≤ 5		134 (59.8%)	59 (54.6%)		103 (56.6%)	90 (60.0%)	
> 5		56 (25.0%)	26 (24.1%)		46 (25.3%)	36 (24.0%)	
NA/ND	13						
Stage	302	204 (100%)	98 (100%)		164 (100%)	138 (100%)	
1		11 (5.4%)	9 (9.2%)	0.360	10 (6.1%)	10 (7.2%)	0.810
2		127 (62.3%)	56 (57.1%)		98 (59.8%)	85 (61.6%)	
3		49 (24.0%)	28 (28.6%)		42 (25.6%)	35 (25.4%)	
4		17 (8.3%)	5 (5.1%)		14 (8.5%)	8 (5.8%)	
NA/ND	43						
Metastasis	342	229 (100%)	113 (100%)		183 (100%)	159 (100%)	
No		144 (62.9%)	83 (74.4%)	0.053	128 (69.9%)	99 (62.3%)	0.138
Yes		85 (37.1%)	30 (25.6%)		55 (30.0%)	60 (37.7%)	
NA/ND	3						
Vital Status	338	225 (100%)	113 (100%)		187 (100%)	151 (100%)	
Died from BC		81 (36.0%)	26 (23.0%)	0.018	51 (27.3%)	56 (37.1%)	0.076
Died from other causes		10 (4.4%)	9 (8.0%)		13 (7.0%)	8 (5.3%)	
Alive		134 (59.6%)	78 (69.0%)		123 (65.7%)	87 (57.6%)	
NA/ND	7						

to bind to the stromal ECM, enabling migration and invasion through adjacent tissues, and ultimately, metastasis [43]. Katoh and collaborators [44] have demonstrated that the ECM protein Tenascin-C (TNC) induces EMT-like phenotypes in breast cancer cells and this mechanism is related with integrin αVβ6 accumulation in focal adhesions. Another body of evidence towards the importance of αV in metastasis comes from studies concerning the role of αVβ3 [45]. Particularly, a work developed by Carter and collaborators have shown that tumor, but not stromal expression of αVβ3 integrin, is essential and required early for spontaneous metastasis, particularly to bone, in triple negative breast cancer models [46]. Our findings that DCIS components present strong staining for integrin αV at their margins, contrasting with invasive lesions, corroborate the work conducted
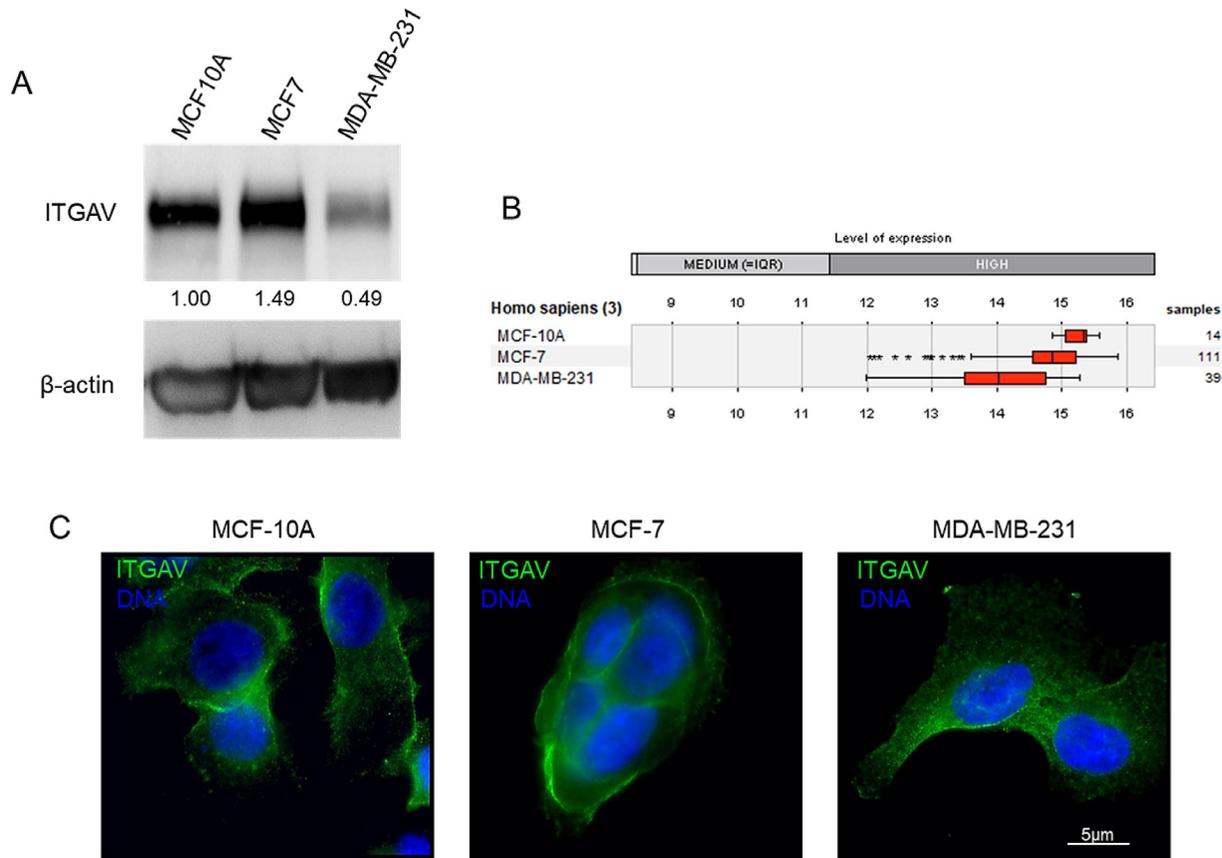
Fig. 5. Integrin αV is less abundant in a human basal-like breast cancer line in comparison to luminal breast cancer or non-tumoral cells. A) Western blot showing the relative amount of integrin αV in sub confluent monolayer cultures of MCF-10A, MCF-7 and MDA-MB231 cell lines. The basal-like cancer cell line MDA-MB231 expresses 50% less integrin αV than the non-tumoral cell line MCF1-0A. The luminal breast cancer cell line MCF-7 still presented high levels of integrin αV. B) *ITGAV* mRNA expression analysis in breast cell lines using the online tool Genevestigator revealed a decrease in *ITGAV* levels for both tumoral cell lines (MCF-7 and MDA-MB231). C) Immunofluorescence of integrin αV (green) in breast cell lines grown as monolayers. Integrin αV fluorescence staining was weaker in the membrane of MDA-MB231 cells. DAPI (blue) was used to stain nuclear DNA. Scale bar = 5 μm.

by Clezardin *et al.*, that found thrombospondin (TSP1) and its receptors (integrin αV and CD36) surrounding *in situ* carcinomas (pure DCIS) [47]. Collectively, our data and the evidence in the literature go along with the notion that, prior to cellular invasion and metastasis, changes have already taken place in regards to the occurrence and behavior of myoepithelial cells, the integrin repertoire expressed by tumor cells, as well as in the ECM molecules available [14,31,48–50].

Our clinicopathological evaluation demonstrated that tumors HER2-negative were associated with the absence of peripheral integrin αV. Of note, IDC associated with DCIS have been shown to be HER2-positive [51]. Also, integrin αV interacts with HER2 in breast cancer cells and can regulate the subcellular localization of HER2, and the combined action of these proteins might influence the invasive phenotype of breast cancer cells [52].

Our cohort has a total of 345 invasive breast cancer cases. Of these, 35 had DCIS components in the TMA sections. On the other hand, an additional analysis comprising only the cases with DCIS versus all cases which were negative for peripheral integrin αV revealed that the presence of the DCIS component per se, without considering the integrin αV staining distribution, was indicative of better clinical outcome (data not shown). Indeed, some reports indicate that breast cancer patients with invasive carcinoma with DCIS components have longer CSS and lower rates of local recurrence [53,54].

Since 3D culture of mammary cell lines recapitulates several aspects of glandular architecture *in vivo* [55–57], we chose this model in order to

establish a parallel with our TMA findings. We performed 3D culture assays using human breast cell lines with different degrees of malignancy: MCF-10A (nonmalignant mammary epithelial), MCF-7 (Luminal-A) and MDA-MB-231 (basal-like). MCF-10A, which is a human breast cell line that retains morphology and biological behavior compatible with differentiated mammary epithelium [55,58], presented a distribution pattern of integrin αV around the acinus, similar to what we found for *in situ* lesions. Contrarily, both tumor cell lines presented integrin αV more evenly distributed in the 3D tumor-like structures, which mimicked our IHC data for invasive lesions, where the peripheral integrin αV is lost, even though it might be present in other areas of the lesion.

The tumor microenvironment (TME) is composed of extracellular matrix (ECM) and multiple non-malignant stromal cells populations, which cooperate with tumor cells in a paracrine and/or through soluble mediators establishing a niche that favors tumor growth [59–62]. Features of the TME components, both cellular and soluble factors, contribute to clinically relevant breast cancer phenotypes and have also been shown to predict patient outcome [27,63,64]. However, unlike other neoplasms such as ovarian [65] and prostate cancer [66], there is no consensus for a soluble marker of prognosis or predictor of treatment in breast cancer, whether bloodstream or even in the tumor microenvironment. Our results indicate that the presence of integrin αV in the stroma is indicative of worsening cancer-specific survival and metastasis free survival rates. Similarly, Smeland and collaborators, suggested that high stromal α11 integrin expression was associated with
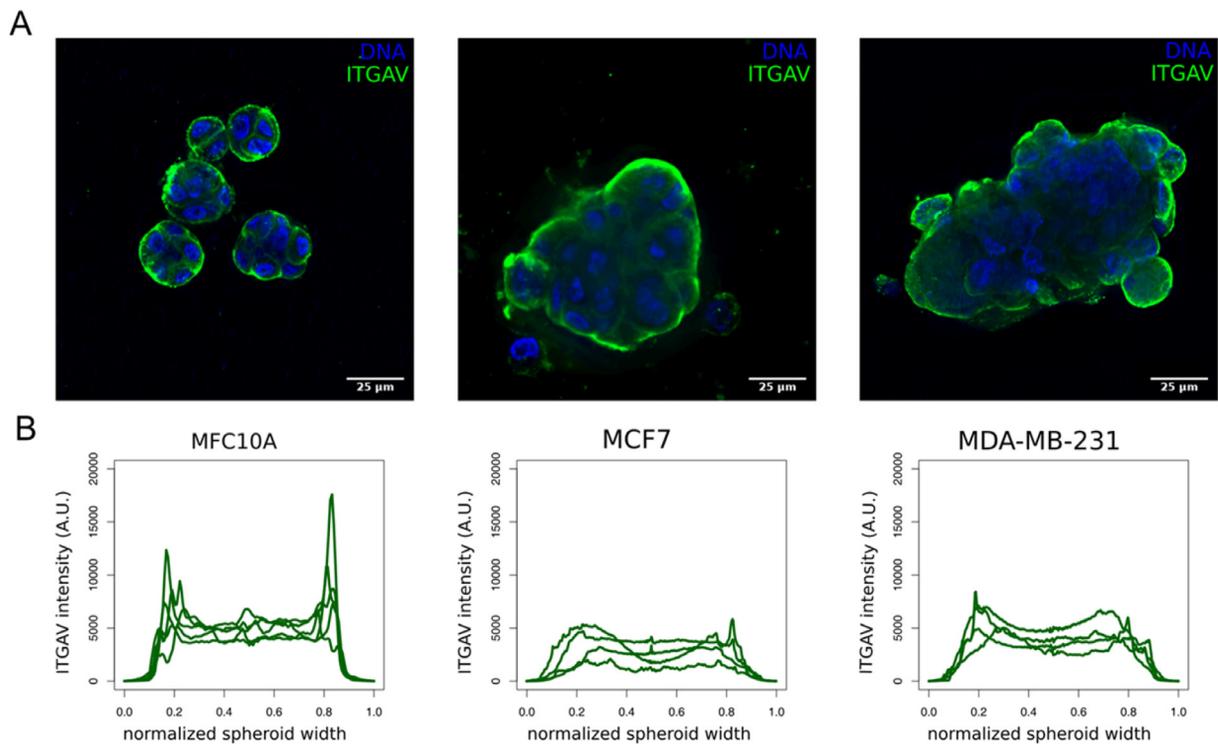
Fig. 6. Three-dimensional structures formed by the human breast cancer cell line MCF-10A (non-malignant) shows higher levels of peripheral integrin αV (ITGAV). A) 3D acini (MCF-10A) and tumor spheroids (MCF-7 and MDA-MB-231) immunostained for integrin αV. B) Fluorescence profile intensity plots of integrin αV of MCF-10A acini ($n = 5$), MCF-7 tumor-spheroids ($n = 4$) and MDA-MB-231 tumor-spheroids ($n = 4$). Scale bar = 25 μm.
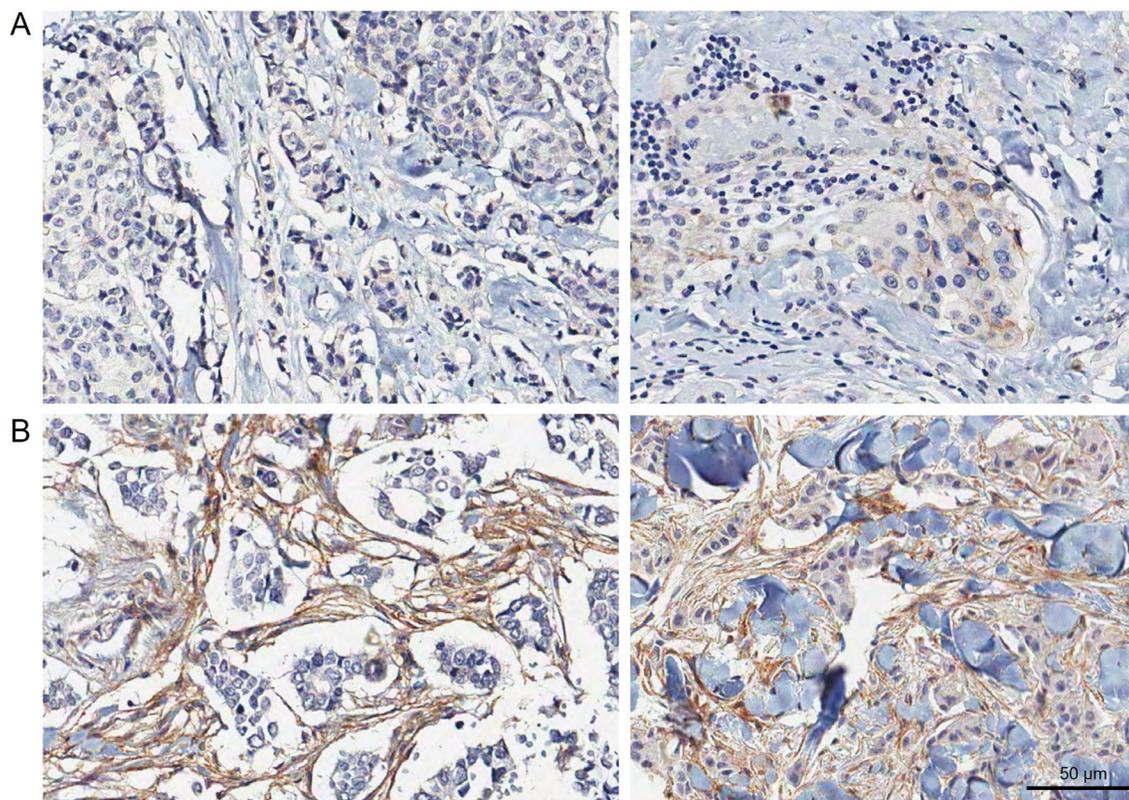
Fig. 7. Representative immunohistochemistry staining images of stromal integrin αV. Breast tissue sections of different lesions arranged in negative stromal integrin αV (A) and positive stromal integrin αv (B). Scale bar = 50 μm.
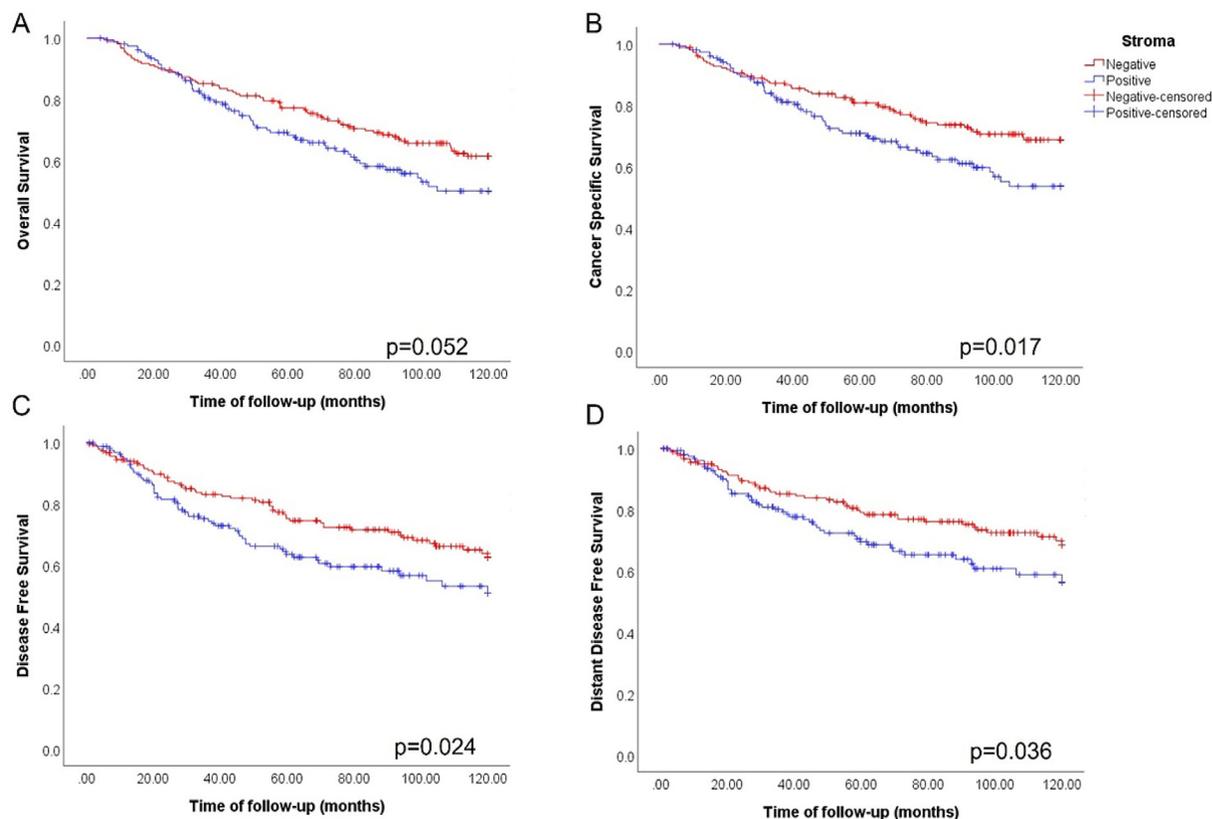
Fig. 8. Presence of stromal integrin αV is associated with metastasis incidence and poor prognosis in human breast tumors. Kaplan-Meier survival curves stratified breast cancer patients of our cohort in negative stromal integrin αV (n=182, red) or positive (n=156, blue): A) For overall survival (OS) no statistical differences were found between the groups (p=0.052). However, in B) the cancer specific survival (CSS) plot shows that patients with positive stromal integrin αV had a worse prognosis when compared to negative stromal integrin αV (p=0.017). Following this trend, we also observe that stromal integrin αV not only worsens the incidence of recurrence C), represented by disease-free survival (DFS) (p=0.024), but also metastases incidence D), showed as distant disease-free survival (DDFS) (p=0.036).

aggressive features of breast cancer. However, this was not associated with breast cancer-specific survival at protein or mRNA levels [63]. Finak *et al.*, using laser capture microdissection to compare gene expression profiles in different tissue tumor regions, proposed a stroma-derived prognostic predictor (SDPP) that stratifies prognosis in breast cancers patient's outcome independently of standard clinical prognostic factors. Among the genes found in the poor outcome profile was integrin subunit beta like 1 (ITGBL1) [67]. Interestingly, in our samples, stromal integrin αV could be identified not only in stromal cells, but also in non-cellular components, in ECM-rich areas. One possible source for these ECM-associated integrins could be extracellular vesicles (EVs), which specific integrin content is believed to be linked to a range of cancer-progression events, including pre-metastatic niche establishment and metastasis organotropism [68]. Particularly, it has been demonstrated that large EVs overexpressing integrin αV contributes to adhesion and invasion in prostate cancer [69]. Furthermore, integrins belong to a large protein family, and alternative splicing can generate more complex and diverse membrane-bound or even truncated/soluble variant integrins [70,71]. Evidence in the literature indicates that soluble isoforms of β3-integrin are strongly associated with tumor cancer metastasis [71–74]. Skaik *et al.*, postulated that secreted β3-integrin can modulate NK cell activity [71]. Although it may be difficult to determine their origin - whether from tumor or stromal cells, associated to EVs or at soluble forms -, targeting integrins in the TME using monoclonal antibodies may be an important therapeutic option to be considered in the future [75,76]. Abergrin (MEDI-522), is an antibody with high affinity to αVβ3 integrin, which is being used in

different clinical trials for prostate cancer (NCT00072930), colorectal cancer (NCT00284817) as well as metastatic melanoma alone or in combination therapy (NCT00111696, NCT00066196) [77]. Collectively, our data point to changes in integrin αV expression patterns in invasive breast cancers, but above all, loss of peripheral localization alongside increased presence in the stroma. Further investigations will be necessary to better elucidate its involvement in tumor progression, as well as its possible use as a prognostic marker in cancer pathology.

Closing Remarks

Taken together, our data indicate that integrin αV localization in breast cancer samples reflects the cell and tissue context, and that the loss of the peripheral layer of integrin αV seems to precede tumor cell invasion. Our work demonstrates that the presence of integrin αV in tumor samples from breast cancer patients could be correlated with either favorable or poor prognosis, depending on the localization pattern within the lesion. Integrin αV at epithelium-stroma interface, which most likely corresponds to myoepithelial cells, is an indicator of a better clinical outcome. Conversely, the presence of integrin αV in the stroma might be an indication of worse prognosis. Thus, we suggest that integrin αV distribution, rather than solely its total mRNA and protein levels, along with other clinical features, could be considered for classification and prognosis in breast cancer.

Author contributions

OLDC, Coordinated TMA assays, harvested and analyzed patient data, performed 2D and 3D cell culture experiments, Western-blot, immunofluorescence, microscopy, data analysis, and manuscript writing.

MCSB contributed with data analysis and statistics.

APZPF contributed with 2D and 3D cell culture experiments, Western-blot, immunofluorescence, microscopy, data analysis as well as manuscript writing and reviewing.

CABTO contributed with supervision in pathology, TMA data generation and analyses.

RT contributed with bioinformatics analysis, manuscript writing and reviewing.

MCCM contributed with image analysis and writing.

RVML contributed with data analysis and statistics.

ECC contributed with IHC assays and writing.

SAVA contributed with patient data harvest and initial statistical analysis.

EMR contributed with the experimental design and supporting grants.

AB-C contributed with planning of experiments, supporting grants, data interpretation and manuscript writing.

Funding information

Conflict of interests

The authors declare no conflict of interest

Acknowledgments

Supplementary materials

Supplementary material associated with this article can be found, in the online version, at doi:10.1016/j.neo.2022.100803.

References

[1] Weigelt B, Peterse JL, van't Veer LJ. Breast cancer metastasis: markers and models. *Nat Rev Cancer* 2005;**5**(8):591–602.

[2] Gumbiner BM. Cell adhesion: the molecular basis of tissue architecture and morphogenesis. *Cell* 1996;**84**(3):345–57.

[3] Takada Y, Ye X, Simon S. The integrins. *Genome Biol* 2007;**8**(5):215.

[4] Van der Flier A, Sonnenberg A. Function and interactions of integrins. *Cell Tissue Res* 2001;**305**(3):285–98.

[5] Geiger B, Bershadsky A. Exploring the neighborhood: adhesion-coupled cell mechanosensors. *Cell* 2002;**110**(2):139–42.

[6] Bissell MJ, Radisky D. Putting tumours in context. *Nat Rev Cancer* 2001;**1**(1):46–54.

[7] Chiarugi P, Giannoni E. Anoikis: a necessary death program for anchorage-dependent cells. *Biochem Pharmacol* 2008;**76**(11):1352–64.

[8] Frisch SM, Ruoslahti E. Integrins and anoikis. *Curr Opin Cell Biol* 1997;**9**(5):701–6.

[9] Frisch SM, Screaton RA. Anoikis mechanisms. *Curr Opin Cell Biol* 2001;**13**(5):555–62.

[10] Moreno-Layseca P, Streuli CH. Signalling pathways linking integrins with cell cycle progression. *Matrix Biol* 2014;**34**:144–53.

[11] Canevari RA, et al. Identification of novel biomarkers associated with poor patient outcomes in invasive breast carcinoma. *Tumour Biol* 2016;**37**(10):13855–70.

[12] Nemeth JA, et al. Alpha-v integrins as therapeutic targets in oncology. *Cancer Invest* 2007;**25**(7):632–46.

[13] Murphy E, Stupack D. Vitronectin-Binding Integrins in Cancer. In: *Cell-extracellular matrix interactions in cancer*. New York, NY: Springer New York; 2010. p. 137–70. R. Zent and A. Pozzi, Editors.

[14] Cerqueira OL, et al. CIP4 promotes metastasis in triple-negative breast cancer and is associated with poor patient prognosis. *Oncotarget* 2015;**6**(11):9397–408.

[15] Lobba, A.R.M., et al., High CD90 (THY-1) expression positively correlates with cell transformation and worse prognosis in basal-like breast cancer tumors. 2018. 13(6): p. e0199254.

[16] Lebeau A, et al. Cellular protein and mRNA expression patterns of matrix metalloproteinases-2, -3 and -9 in human breast cancer: correlation with tumour growth. *J Mol Histol* 2004;**35**(5):443–55.

[17] Hong SW, et al. Matrix metalloproteinase-2 and -7 expression in colorectal cancer. *J Korean Soc Coloproctol* 2011;**27**(3):133–9.

[18] Jahkola T, et al. Tenascin-C expression in invasion border of early breast cancer: a predictor of local and distant recurrence. *Br J Cancer* 1998;**78**(11):1507–13.

[19] Lowy CM, Oskarsson T. Tenascin C in metastasis: a view from the invasive front. *Cell Adh Migr* 2015;**9**(1-2):112–24.

[20] Wolff AC, et al. Human epidermal growth factor receptor 2 testing in breast cancer: American Society of Clinical Oncology/College of American Pathologists clinical practice guideline focused update. *Arch Pathol Lab Med* 2018.

[21] Kenny PA, et al. The morphologies of breast cancer cell lines in three-dimensional assays correlate with their profiles of gene expression. *Mol Oncol* 2007;**1**(1):84–96.

[22] Schindelin J, et al. Fiji: an open-source platform for biological-image analysis. *Nat Methods* 2012;**9**(7):676.

[23] Madden SF, et al. BreastMark: an integrated approach to mining publicly available transcriptomic datasets relating to breast cancer outcome. *Breast Cancer Res* 2013;**15**(4):R52.

[24] Hruz T, et al. Genevestigator v3: a reference expression database for the meta-analysis of transcriptomes. *Adv Bioinformatic* 2008 **2008**.

[25] Zarrella ER, et al. Automated measurement of estrogen receptor in breast cancer: a comparison of fluorescent and chromogenic methods of measurement. *Lab Invest* 2016;**96**(9):1016.

[26] Denadai MV, et al. Expression of integrin genes and proteins in progression and dissemination of colorectal adenocarcinoma. *BMC Clin Pathol* 2013;**13**:16.

[27] de Kruijf E, et al. Tumor-Stroma Ratio within the Primary Tumor Is a Prognostic Factor in Early Breast Cancer Patients, Especially in Triple-Negative-Carcinoma Patients. *Cancer Res* 2009;**69**(24 Supplement):3049.

[28] Schittenhelm J, et al. Longitudinal expression analysis of alphav integrins in human gliomas reveals upregulation of integrin alphavbeta3 as a negative prognostic factor. *J Neuropathol Exp Neurol* 2013;**72**(3):194–210.

[29] Waisberg J, et al. Overexpression of the ITGAV gene is associated with progression and spread of colorectal cancer. *Anticancer Res* 2014;**34**(10):5599–607.

[30] Koukoulis G, et al. Immunohistochemical localization of integrins in the normal, hyperplastic, and neoplastic breast. Correlations with their functions as receptors and cell adhesion molecules. *Am J Pathol* 1991;**139**(4):787.

[31] Ronnov-Jessen L, Petersen OW, Bissell MJ. Cellular changes involved in conversion of normal to malignant breast: importance of the stromal reaction. *Physiol Rev* 1996;**76**(1):69–125.

[32] Greenbaum D, Jansen R, Gerstein M. Analysis of mRNA expression and protein abundance data: an approach for the comparison of the enrichment of features in the cellular population of proteins and transcripts. *Bioinformatics* 2002;**18**(4):585–96.

[33] Ideker T, et al. Integrated genomic and proteomic analyses of a systematically perturbed metabolic network. *Science* 2001;**292**(5518):929–34.

[34] Greenbaum D, et al. Comparing protein abundance and mRNA expression levels on a genomic scale. *Genome Biol* 2003;**4**(9):117.

[35] Tian Q, et al. Integrated genomic and proteomic analyses of gene expression in mammalian cells. *Mol Cell Proteomics* 2004;**3**(10):960–9.

[36] Brockmann R, et al. Posttranscriptional expression regulation: what determines translation rates? *PLoS Comput Biol* 2007;**3**(3).

[37] Mata J, Marguerat S, Bähler J. Post-transcriptional control of gene expression: a genome-wide perspective. *Trends Biochem Sci* 2005;**30**(9):506–14.

[38] Gudjonsson T, et al. Myoepithelial cells: their origin and function in breast morphogenesis and neoplasia. *J Mammary Gland Biol Neoplasia* 2005;**10**(3):261–72.

[39] Fiore APZP, et al. Laminin-111 and the level of nuclear actin regulate epithelial quiescence via exportin-6. *Cell Rep* 2017;**19**(10):2102–15.

[40] Fiore APZP, de Freitas Ribeiro P, Bruni-Cardoso A. Sleeping beauty and the microenvironment enchantment: microenvironmental regulation of the proliferation-quiescence decision in normal tissues and in cancer development. *Front Cell Dev Biol* 2018;**6**.

[41] Ensslin MA, Shur BD. The EGF repeat and discoidin domain protein, SED1/MFG-E8, is required for mammary gland branching morphogenesis. *Proc Natl Acad Sci* 2007;**104**(8):2715–20.

[42] Sternlicht MD, et al. The human myoepithelial cell is a natural tumor suppressor. *Clin Cancer Res* 1997;**3**(11):1949–58.

[43] Pelaez R, et al. Integrins: moonlighting proteins in invadosome formation. *Cancers (Basel)* 2019;**11**(5).

[44] Katoh D, et al. Binding of αvβ1 and αvβ6 integrins to tenascin-C induces epithelial–mesenchymal transition-like change of breast cancer cells. *Oncogenesis* 2013;**2**:e65.

[45] Kwakwa KA, Sterling JA. Integrin alphavbeta3 Signaling in Tumor-Induced Bone Disease. *Cancers (Basel)* 2017;**9**(7).

[46] Carter RZ, et al. Tumour but not stromal expression of β 3 integrin is essential, and is required early, for spontaneous dissemination of bone-metastatic breast cancer. *J Pathol* 2015;**235**(5):760–72.

[47] Clezardin P, et al. Expression of thrombospondin (TSP1) and its receptors (CD36 and CD51) in normal, hyperplastic, and neoplastic human breast. *Cancer Res* 1993;**53**(6):1421–30.

[48] Truesdell P, et al. CIP4 promotes lung adenocarcinoma metastasis and is associated with poor prognosis. *Oncogene* 2014;**34**:3527.

[49] Lebeau A, et al. Cellular protein and mRNA expression patterns of matrix metalloproteinases-2,-3 and-9 in human breast cancer: correlation with tumour growth. *J Mol Histol* 2004;**35**(5):443–55.

[50] Jahkola T, et al. Expression of tenascin in invasion border of early breast cancer correlates with higher risk of distant metastasis. *Int J Cancer* 1996;**69**(6):445–7.

[51] Wong H, et al. Presence of an in situ component is associated with reduced biological aggressiveness of size-matched invasive breast cancer. *Br J Cancer* 2010;**102**(9):1391–6.

[52] Lal S, et al. Interactions between alphav-Integrin and HER2 and Their Role in the Invasive Phenotype of Breast Cancer Cells In Vitro and in Rat Brain. *PLoS One* 2015;**10**(7):e0131842.

[53] Cedolini C, et al. Impact of the presence and quantity of ductal carcinoma in situ component on the outcome of invasive breast cancer. *Int J Clin Exp Pathol* 2015;**8**(10):13304–13.

[54] Logullo AF, et al. Presence of ductal carcinoma in situ confers an improved prognosis for patients with T1N0M0 invasive breast carcinoma. *Braz J Med Biol Res* 2002;**35**(8):913–19.

[55] Debnath J, Muthuswamy SK, Brugge JS. Morphogenesis and oncogenesis of MCF-10A mammary epithelial acini grown in three-dimensional basement membrane cultures. *Methods* 2003;**30**(3):256–68.

[56] Strauss BE, et al. Perspectives for cancer immunotherapy mediated by p19Arf plus interferon-beta gene transfer. *Clinics (Sao Paulo)* 2018;**73**(suppl 1):e479s.

[57] Debnath J, et al. The role of apoptosis in creating and maintaining luminal space within normal and oncogene-expressing mammary acini. *Cell* 2002;**111**(1):29–40.

[58] do Amaral JB, et al. MCF-7 cells as a three-dimensional model for the study of human breast cancer. *Tissue Eng Part C Methods* 2011;**17**(11):1097–107.

[59] Dvorak HF. Tumors: wounds that do not heal. Similarities between tumor stroma generation and wound healing. *N Engl J Med* 1986;**315**(26):1650–9.

[60] Dvorak HF. Tumors: wounds that do not heal-redux. *Cancer Immunol Res* 2015;**3**(1):1–11.

[61] Maman S, Witz IP. A history of exploring cancer in context. *Nat Rev Cancer* 2018;**18**(6):359–76.

[62] Pietras K, Östman A. Hallmarks of cancer: interactions with the tumor stroma. *Exp Cell Res* 2010;**316**(8):1324–31.

[63] Smeland HY-H, et al. Integrin α11β1 is expressed in breast cancer stroma and associates with aggressive tumor phenotypes. *J Pathol* 2020;**6**(1):69–82.

[64] Medrek C, et al. The presence of tumor associated macrophages in tumor stroma as a prognostic marker for breast cancer patients. *BMC Cancer* 2012;**12**:306.

[65] Bonifácio VDB. Ovarian cancer biomarkers: moving forward in early detection. *Adv Exp Med Biol* 2020;**1219**:355–63.

[66] Saini S. PSA and beyond: alternative prostate cancer biomarkers. *Cell Oncol (Dordr)* 2016;**39**(2):97–106.

[67] Finak G, et al. Stromal gene expression predicts clinical outcome in breast cancer. *Nat Med* 2008;**14**(5):518–27.

[68] Grigoryeva ES, et al. Do tumor exosome integrins alone determine organotropic metastasis? *Mol Biol Rep* 2020;**47**(10):8145–57.

[69] Ciardiello C, et al. Large oncosomes overexpressing integrin alpha-V promote prostate cancer adhesion and invasion via AKT activation. *J Exp Clin Cancer Res* 2019;**38**(1):317.

[70] Blencowe BJ. Alternative splicing: new insights from global analyses. *Cell* 2006;**126**(1):37–47.

[71] Skaik Y, et al. Secreted β3-integrin enhances natural killer cell activity against acute myeloid leukemia cells. *PLoS One* 2014;**9**(2):e98936.

[72] Lonsdorf AS, et al. Engagement of αIIbβ3 (GPIIb/IIIa) with αvβ3 integrin mediates interaction of melanoma cells with platelets: a connection to hematogenous metastasis. *J Biol Chem* 2012;**287**(3):2168–78.

[73] Jin R, et al. A naturally occurring truncated beta3 integrin in tumor cells: native anti-integrin involved in tumor cell motility. *Cancer Biol Ther* 2007;**6**(10):1559–68.

[74] Djaffar I, et al. A new alternative transcript encodes a 60 kDa truncated form of integrin beta 3. *Biochem J* 1994;**300**(Pt 1):69–74 Pt 1.

[75] Hamidi H, Ivaska J. Every step of the way: integrins in cancer progression and metastasis. *Nat Rev Cancer* 2018;**18**(9):533–48.

[76] Abdollahi A, et al. Inhibition of alpha(v)beta3 integrin survival signaling enhances antiangiogenic and antitumor effects of radiotherapy. *Clin Cancer Res* 2005;**11**(17):6270–9.

[77] Hofmeister V, Schrama D, Becker JC. Anti-cancer therapies targeting the tumor stroma. *Cancer Immunol Immunother,* 2008;**57**(1):1–17.